Pulverized Coal Combustion Application of Laser-Based Temperature Sensing System using Computed Tomography - Tunable Diode Laser Absorption Spectroscopy(CT-TDLAS)

Zhenzhen Wang[a,b], Yoshihiro Deguchi[a,b*], Takahiro Kamimoto[b], Kazuki Tainaka[c], Kenji Tanno[c]

[a]State Key Laboratory of Multiphase Flow in Power Engineering, Xi'an Jiaotong University, Xi'an 710049, China

[b]Graduate School of Advanced Technology and Science, Tokushima University, Tokushima 770-8501, Japan

[c]Central Research Institute of Electric Power Industry, Nagasaka, Yokosuka, Kanagawa, 240-019, Japan

[*]Corresponding author: Email address: ydeguchi@tokushima-u.ac.jp

Abstract

The investigation of combustion phenomena in pulverized coal flames is significant for combustion optimization related to energy conservation and emission reduction. Real-time two dimensional (2D) temperature and concentration distributions play an important role for combustion analysis. The non-contact and fast response 2D temperature and concentration distribution measurement method was developed in this study. The method is based on a combination of computed tomography (CT) and tunable diode laser absorption spectroscopy (TDLAS). The accuracy evaluation of developed 32-path CT-TDLAS demonstrated its feasibility of 2D temperature measurement. 32-path CT-TDLAS was applied to CH_4 and 5 kg/h coal combustion fields for 2D temperature measurement. The time-series 2D temperature distribution in coal combustion furnace was measured using 32-path CT-TDLAS measurement cell with kHz time resolution. The transient temperature field of combustion flame directly reflects the combustion mode and combustion stability. The measurement results demonstrate its applicability of CT-TDLAS to various types of combustor, especially the combustion fields with coal and ash particles. CT-TDLAS method with kHz response time enables the real-time 2D temperature measurement to be applicable for combustion analysis.

Keywords: Coal combustion; 2D temperature measurement; Time-series distribution; Tunable diode laser absorption spectroscopy (TDLAS); Computed tomography (CT)

1. Introduction

The fossil fuel, such as coal, oil and natural gas, is the major source of energy. The energy and environment issues have become a global concern. The long-term energy consumption is dominated by coal in China. The safety, high-efficiency and low pollution are significant for coal combustion. Therefore, investigation of combustion phenomena in pulverized coal flames is important for combustion optimization with the development of efficient coal burners and improvement of numerical simulation models. However, the acquisition of vital combustion parameters is the key to combustion optimization. The temperature distribution is closely related to the combustion efficiency, gas pollutants emission, unburned carbon loss, and so on. Especially, real-time two dimensional (2D) temperature and species concentration distributions play an important role for combustion field analysis. Traditional contact measurement methods can not realize real-time online monitoring due to some limitations of temperature range, distribution point, etc.

Recently, laser diagnosis has been developed and applied for actual industrial fields due to its features of non-contact, high sensitivity and fast response [1,2]. Tunable diode laser absorption spectroscopy (TDLAS) has been developed for temperature and species concentration measurement in gas turbine, coal gasifier, process control and environment monitoring using absorption spectra of molecules such as H_2O, NH_3 and CH_4 [3-6]. With engineering development, the transient phenomena of start-ups and load changes in engines have been elucidated in various conditions gradually [7]. A chemical species tomography scheme, which was amenable to replication for many simultaneous measurement channels, was applied for simultaneous measurement of multiple species [8]. The combination method of computed tomography-tunable diode laser absorption spectroscopy (CT-TDLAS) based on computed tomography (CT) and TDLAS has also been developed for 2D temperature and species concentration measurement in automotive engine and aero-propulsion engine [9-11]. Various tomographic reconstruction methods have been investigated. 2D temperature and NH_3 concentration were measured using a cylindrical retro-reflector with the algebraic reconstruction technique (ART) [12]. The hyperspectral absorption spectroscopy method was developed to increase spectral information for simultaneous reconstruction of temperature and species concentration [13-15]. In order to simultaneously retrieve distributions of temperature, species concentration and pressure, a technique based on broad bandwidth and frequency-agile tomographic absorption spectroscopy was also proposed for the study of dynamic combustion flows [16]. The 16-path CT-TDLAS method was applied to the oscillating flames and Bunsen type burner for time-series 2D temperature and CH_4 concentration distributions [17,18]. Various spatial resolution quantification approaches have also been discussed to evaluate the spatial resolution [19]. Due to the kHz response time of CT-TDLAS, the method enables real-time 2D temperature and species concentration measurement, which is applicable for the combustion analysis. However, it has been still difficult to accomplish in-situ measurement of temperature and species concentration in coal combustion fields because of the existing coal and ash particles in combustion fields.

In this study, a fast response 2D temperature and concentration measurement method was developed and applied to coal combustion field. The technique is based on a CT method using absorption spectra of H_2O molecule. The CT-TDLAS method using 32-path configuration was applied to measure time-series 2D temperature distribution in a 5 kg/h pulverized coal furnace for the first time. The novel CT algorism using 2D polynomials for temperature and concentration distributions was developed to improve CT reconstruction performance. According to the 2D temperature measurement results, the coal combustion can be analyzed. The CT-TDLAS application for time-series 2D temperature measurement in coal combustion field demonstrates its applicability for severe environment, such as high temperature, high dust, high moisture, corrosivity, etc.

2. Theory

2.1 CT-TDLAS

Gas temperature and species concentration can be determined according to the measurement of molecular absorbance at multiple wavelengths using TDLAS, which is possible to scan laser wavelength continuously and detect absorption spectra. TDLAS technique is based on Lambert Beer's law. The intensity of permeated light is related to absorber concentration when laser light permeates an absorption medium [1]. The direct absorption spectroscopy was employed using kHz wavelength scanning, which shows more distinct spectral evaluation than that of sinusoidal modulation. Figure 1 shows the concept of direct absorption spectroscopy at different conditions. When the laser intensity is attenuated by dirt on windows, vibration, and/or scattering by particles, the absorption intensity can be normalized by the laser intensity measured in each wavelength scanning. The laser intensity fluctuation does not affect the accuracy of measurement and it is often called "self-calibration" [1]. Temperature can be measured by evaluating several absorption lines from same molecule with different temperature dependence [18,20], which is also important to reduce the temperature error induced by CT algorism. In this study, H_2O absorption spectra around 1388nm and 1343nm were used to measure the temperature.

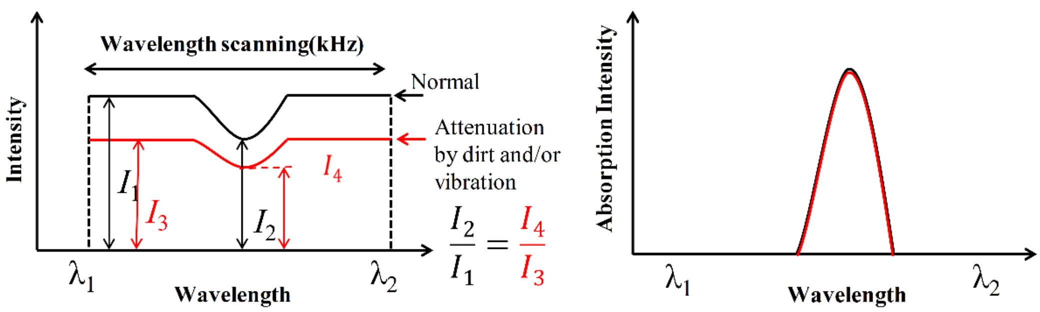

(a) Wavelength scanning (b) Absorption intensity

Figure 1 Concept of direct absorption spectroscopy

The absorption signal intensity of transmitted light through absorption medium becomes an integrated value along the optical path. Various optical paths can be intersected to each other to configurate the optical grids for 2D distribution reconstruction by a CT method. 32-path laser beams configuration and its 32-path CT algorithm were used to measure 2D temperature distribution in this study. Concept of laser beam paths and CT algorithm flow chart is shown in Figure 2. The integrated absorbance of $A_{\lambda,p}$ depends on both temperature and concentration. Therefore, the temperature should be calculated by more than two different absorbance values. In this study, the theoretical H_2O spectroscopic database [21] has been corrected under various temperature and pressure conditions to improve its measurement accuracy. A set of measured H_2O absorption spectra is compared to the theoretical spectra with the corrected spectroscopic database. In order to minimize the spectra fitting error, the temperature and H_2O concentration at each analysis position are determined using a multi-function minimization method. Sets of temperature and concentration distributions at analysis position can be determined simultaneously shown in Figure 2. The set of temperature and concentration is determined to minimize the total error, which is evaluated by the spectra fitting method. A polynomial noise reduction technique is also used to reduce noises such as the effect of laser beam steering [7]. The spectra fitting method and polynomial noise reduction technique are significant to acquire the stable and accurate CT reconstruction.

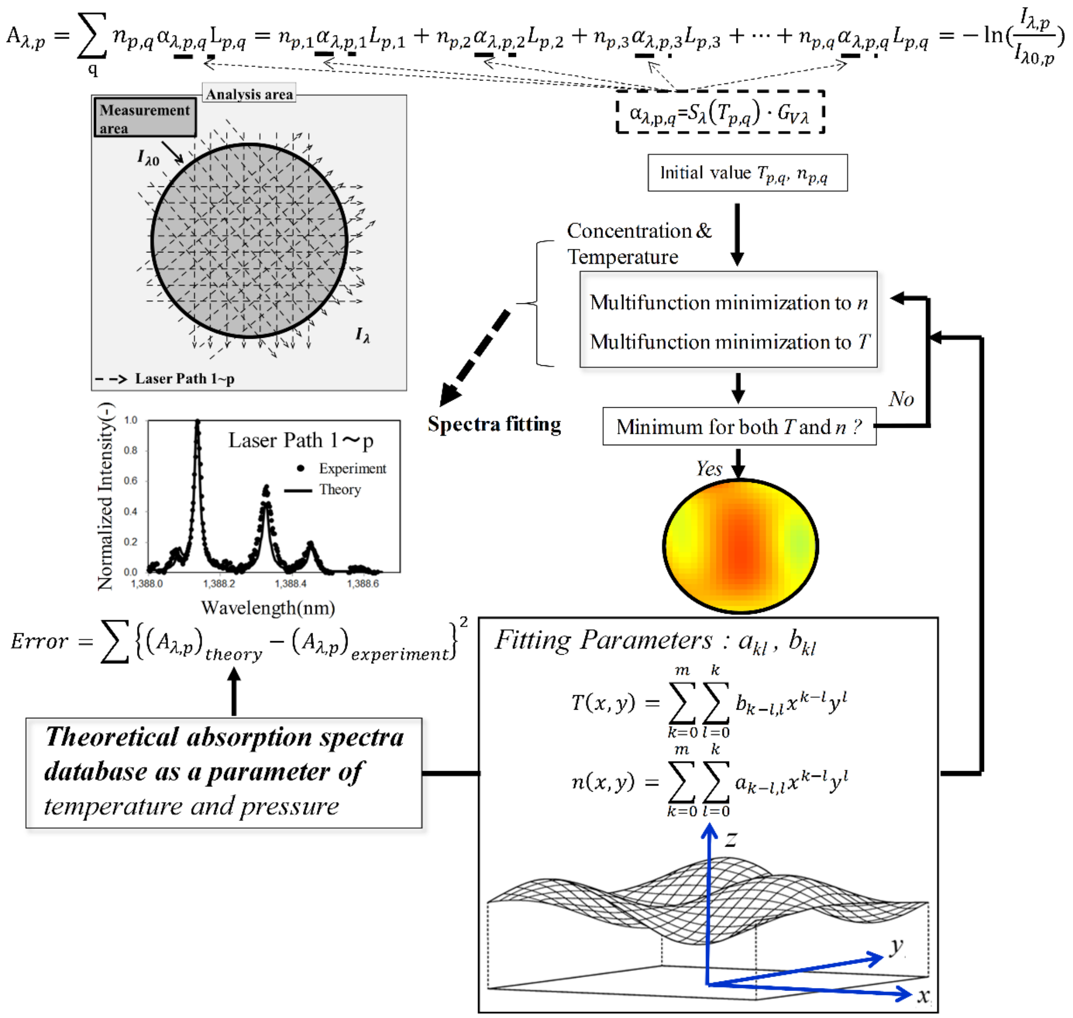

Figure 2 Laser beam paths and CT algorithm

This novel CT algorism is developed to realize the stable CT reconstruction calculation. The 2D temperature and concentration distributions are defined by the 2D polynomials for T(x,y) and n(x,y) when employing the fitting parameters of a_{kl} and b_{kl}. 2D temperature and concentration information is used to calculate the absorption coefficient at each position. The error minimization is performed as a function of the polynomial parameters a and b. Using this method, spatial resolution of temperature and concentration distribution can be determined by the polynomial order m and interval between calculated positions can be minimized arbitrarily. One of the most prominent merits of this method is its stability of reconstruction especially at the edge of measurement area where the laser path number is usually small compared to the centre one. This is because the spatial resolution of temperature and concentration distribution is determined by the polynomial order and is not determined locally by the axes of the measurement area. The downhill simplex [22] and Levenberg-Marquardt methods for multifunction minimization were used in this study.

2.2 Image analysis

CT-TDLAS can reconstruct a 2D temperature distribution image using the absorption spectra. In order to verify the accuracy of CT reconstruction, the sum of squared difference (SSD) and zero-mean normalized cross-correlation (ZNCC) between the original profile and the CT reconstructed profile are compared and analyzed. The approaches were described elsewhere in detail [23,24]. SSD is the area range of reconstructed pattern in the image by comparing the sum of squared difference between the pixels of specified area and the pixels of target pattern. If the SSD value is closer to "0", the error between original profile and CT reconstructed profile is smaller with almost same values of two profiles. ZNCC is a zero-mean normalized cross-correlation, which represents a correlation between original profile and CT reconstructed profile. If the ZNCC value is closer to "1", the correlation between two profiles is higher with almost same patterns. Equations (1) and (2) define the SSD value and ZNCC value.

$$SSD = \sqrt{\frac{\sum_{x=0}^{X-1}\sum_{y=0}^{Y-1}\left[\left(T_{x,y}\right)_{original} - \left(T_{x,y}\right)_{CT-TDLAS}\right]^2}{XY}} \Big/ T_R \quad (1)$$

$$ZNCC=\frac{\sum_{x=0}^{X-1}\sum_{y=0}^{Y-1}\left[\left(T_{x,y}-\bar{T}\right)_{original}\cdot\left(T_{x,y}-\bar{T}\right)_{CT-TDLAS}\right]}{\sqrt{\sum_{x=0}^{X-1}\sum_{y=0}^{Y-1}\left(T_{x,y}-\bar{T}\right)_{original}\cdot\sum_{x=0}^{X-1}\sum_{y=0}^{Y-1}\left(T_{x,y}-\bar{T}\right)_{CT-TDLAS}^{2}}} \quad (2)$$

$$\bar{T}=\frac{\sum_{x=0}^{X-1}\sum_{y=0}^{Y-1}T_{x,y}}{XY} \quad (3)$$

Where, $T_{x,y}$ is the temperature at each position in calculated area. T_R is the representing temperature and was set to be 1800K in this study. X is the total number of meshes along x-axis in calculated area, and Y is the total number of meshes along y-axis in calculated area.

In this study, the image differences between original profile and its CT reconstructed profile were compared to evaluate the CT reconstruction accuracy of employed 32-path configuration. The original profiles were simulated by an assumed temperature distribution and three computational fluid dynamics (CFD) results.

3. Experimental setup

CT-TDLAS was applied to pulverized coal combustion furnace with coal feed rate of 5 kg/h to measure the time-series 2D temperature distribution in pulverized coal flame in this study. Figure 3 shows the experimental apparatus of pulverized coal combustion field measurement using CT-TDLAS. The experimental system mainly consisted of the combustion furnace with coal burner and pilot methane (CH_4) burner, the CT-TDLAS measurement cell, as well as their related components, as shown in Figure 3(a). The combustion furnace was a vertical cylinder with an inner diameter of 250 mm and height of 2300 mm. The coal burner was a triple concentric jet burner, which may become hot because of the radiation from particles. The primary, secondary, and tertiary air were used for feeding coal, protecting coal burner from radiation heat, and supplying combustion air, respectively. Inner diameters of the coal burner were 5.7 mm, 44.6 mm, and 52.5 mm in order. In addition, entrainment air was supplied to prevent flowing back. The experimental conditions of CH_4 flame and pulverized coal flame were summarized in Table 1. The CT-TDLAS measurement cell was installed at the plane of 595 mm from the coal burner inside, as illustrated in Figure 3(b).

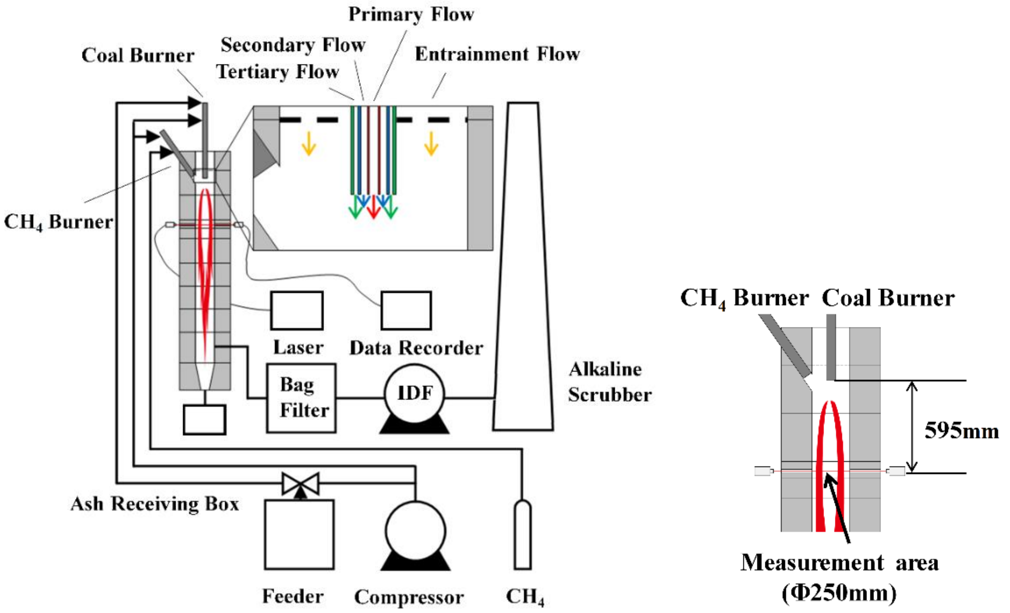

(a) Experimental system (b) Measurement plane

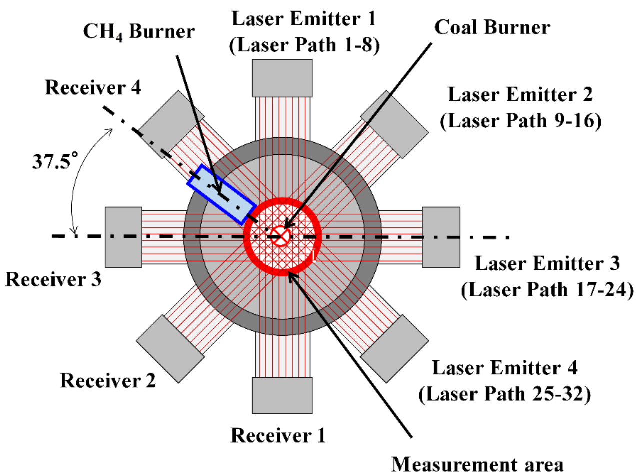

(c) 32-path CT configuration

Figure 3 Experimental apparatus of pulverized coal combustion field measurement using CT-TDLAS

Table 1 Experimental conditions of CH_4 and pulverized coal flames

	Condition	CH_4 fuel	CH_4+Coal fuel
Coal burner	Coal feed rate [kg/h]	-----	5
	Primary air flow rate [L_N/min]	-----	39
	Secondary air flow rate [L_N/min]	-----	20
	Tertiary air flow rate [L_N/min]	-----	138
	Entrainment air flow rate [L_N/min]	-----	198
	Air-fuel ratio [-]	-----	1.1
CH_4 burner	CH_4 flow rate [L_N/min]	30.0	30.0
	Air flow rate [L_N/min]	320.0	320.0

Temperature measurement using CT-TDLAS was performed using H_2O absorption spectra. The wavelengths of diode lasers (NTT Electronics Co., NLK1E5GAAA/NLK1B5EAAA) were from 1388.0 to 1388.6 nm and from 1342.9 to 1343.5 nm, which were employed to maintain the sufficient measurement accuracy at low and high temperature [17,18]. The wavelength scanning rate was 4 kHz. The two wavelength laser beams were mixed using the fiber combiner and the mixed laser beam was separated by an optical fiber splitter (OPNETI CO., SMF-28e 1310 nm SWBC 2×32) to 32 paths. The separated laser beams irradiated into the flame by 32 collimators. The transmitted laser intensities were detected by 32 photodiodes after passing through the flame and then recorded by analyzer including 32 amplifiers and recorder. In order to eliminate the radiation effect, the filter (SIGMA KOKI CO., VPF-05C-08P-T1340/1390-R825/1600) with the transmittance specification of 1340-1390 nm>95%, 500-1250 nm<2%, 1500-2000 nm<2% was utilized with the detectors. As optical access ports, 32 collimators and 32 detectors were embedded in the 32-path CT-TDLAS measurement cell. Figure 3(c) shows the designed 32-path CT configuration of measurement cell with four sets of laser emitters and four sets of receivers. The 32 laser paths in the measurement cell were purged using 40 L_N/min nitrogen (N_2) flow to eliminate H_2O absorption in the interlayer of measurement cell.

4. Results and discussion

32-path CT-TDLAS measurement method for 2D temperature measurement was used in pulverized coal combustion field. One of the important aspects for CT-TDLAS application is the accuracy evaluation of CT-TDLAS. Therefore, the accuracy of employed 32-path CT-TDLAS measurement method was discussed to verify its reliability before the measurement of 2D temperature distribution of pulverized coal flame using CT-TDLAS.

4.1 Accuracy evaluation of CT-TDLAS

The accuracy of CT-TDLAS measurement method should be evaluated in two parts. The temperature measurement accuracy of TDLAS and the 2D reconstruction accuracy of 32-path CT-algorithm were evaluated respectively in this study.

4.1.1 Accuracy evaluation of TDLAS

In this method, for the temperature measurement using H_2O absorption spectra, the theoretical H_2O spectroscopic database has been corrected under various temperature and pressure conditions to improve TDLAS measurement accuracy. The consistency of theoretical absorption spectra and experimental absorption spectra was improved significantly when employing the corrected spectroscopic database [18,25]. The temperature from 300 to 2000 K of a flat flame burner and a high-temperature and high-pressure measurement cell was measured by TDLAS and thermocouple to verify the temperature measurement accuracy of TDLAS [18]. The comparison of measured temperature between TDLAS and thermocouple is shown in Figure 4 and Table 2 under different temperature conditions. The temperature measured by TDLAS was calculated using the uncorrected spectroscopic database and corrected spectroscopic database, respectively. The measured temperature by TDLAS using corrected spectroscopic database showed the improved linearity with the measured temperature by thermocouple, as shown in Figure 4. Table 2 lists the temperature difference between thermocouple and TDLAS with corrected spectroscopic database, which shows that the maximum difference was 32.5 K and the maximum error was 2.3% in the measured temperature range from 300 to 2000 K. Therefore, the correction of spectroscopic database is necessary to improve the temperature measurement accuracy for TDLAS technique.

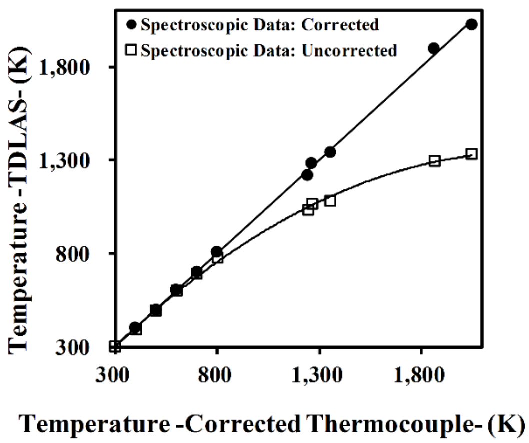

Figure 4 Temperature comparison between thermocouple and TDLAS with/without corrected spectroscopic database

Table 2 Temperature difference between thermocouple and TDLAS with corrected spectroscopic database

Thermocouple (K)	TDLAS with correction (K)	Temperature difference (K)	Error
300	299.9	-0.1	0.0%
400	398.9	-1.1	0.3%
500	498.9	-1.1	0.2%
600	604.0	4.0	0.7%
700	699.8	-0.2	0.0%
800	803.3	3.3	0.4%
1244	1215.0	-29.0	2.3%
1264	1282.3	18.4	1. 5%
1354	1340.0	-14.0	1.0%
1864	1896.5	32.5	1.7%
2048	2021.5	-26.6	1.3%

4.1.2 Accuracy evaluation of 32-path CT reconstruction

The accuracy of CT reconstruction can be evaluated using the assumed temperature distribution and/or CFD result of temperature distribution. In this study, the image differences given by an assumed temperature profile and its corresponding CT reconstructed profile of 32-path configuration were discussed to evaluate the 2D reconstruction accuracy of 32-path CT-algorithm. Three CFD results of temperature distribution were also used to evaluate the accuracy of 32-path CT reconstruction.

An assumed temperature distribution based on centrosymmetric Cauchy distribution was used first, as shown in Figure 5(a). Figure 5 shows the comparison between the assumed temperature distribution with high temperature region in center and its 32-path CT reconstructed result. The reconstructed profile shows the accordant temperature distribution with the original profile according to Figure 5(a) and Figure 5(b). The temperature distributions at Y=0mm, 60deg and 120deg were compared between original distribution and CT reconstructed results, which shows some difference at the region around X=Y=0mm in Figure 5(c). Because of the limited number of paths, the temperature change with large curvature cannot be reconstructed correctly by the employed 32-path configuration. The accuracy of CT reconstruction can be improved when increasing the paths, which depends on the actual situation of applications. Figure 5(d) shows the comparison of curvature at Y=0mm. The maximum curvature of the CT reconstructed result was 0.04 mm^{-1}. If the spatial resolution was defined using the radius of curvature, the spatial resolution of this method was determined to 25 mm. The spatial resolution can be improved when increasing the laser path. If using 64 paths, the spatial resolution becomes to be 12 mm evaluated by the maximum curvature.

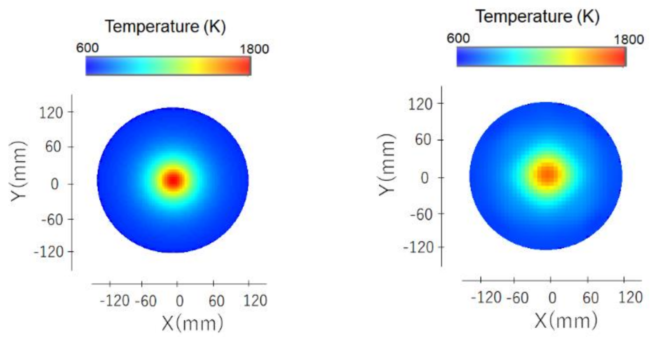

(a) Assumed temperature 1 (b) CT reconstruction 1

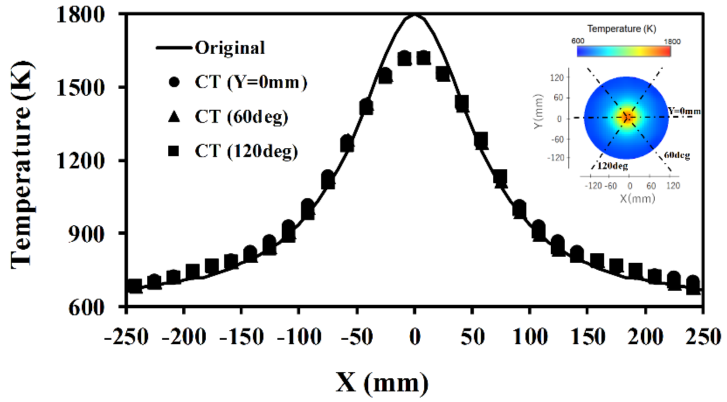

(c) Comparison of temperature distributions at Y=0mm, 60deg and 120deg

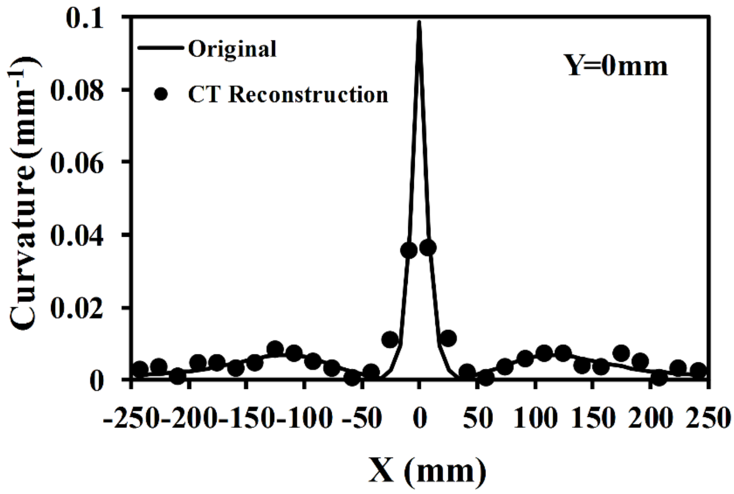

(d) Comparison of curvature at Y=0mm

Figure 5 Comparison of temperature distributions between assumed temperature and reconstructed temperature by 32-path CT-algorithm

A numerical simulation of a pulverized coal flame for temperature distribution was performed with working model sets by Large Eddy Simulation (LES) technique using NuFD/FrontFlowRed (FFR-Comb). The employed gas-particle two-phase reacting flow LES solver was unstructured and based on Finite Volume Method (FVM) with massively parallel computing code. The turbulence model and combustion model were dynamic Smagorinsky and scale similarity filtered reaction rate models for flow field. As for particle motion, coal particles were traced in the Lagrangian method individually. The field model was employed as the combustion model. The boundary condition was adiabatic for simulation. The detailed description of pulverized coal combustion simulation was reported elsewhere [26-28]. These simulated temperature distributions were also reconstructed according to the 32-path configuration. Figure 6 shows the comparison between three CFD temperature distributions and their CT reconstructions. These results were good enough to be considered as almost the same profiles. Therefore, it is demonstrated that the CT reconstructed distribution in the measured area agreed well with the original distribution. In Figure 5 and Figure 6, the CT reconstructed distributions spread more widely than these of the assumed and CFD distributions due to the calculation of CT reconstruction based on limited number of absorbance. Table 3 lists SSD and ZNCC for these four reconstructed cases. The SSD value is closer to "0" and the ZNCC value is closer to "1", which demonstrate smaller error and higher correlation of two profiles. SSD and ZNCC in Table 3 show reasonable results to verify the CT reconstruction accuracy.

Table 3 SSD and ZNCC of 32-path CT-algorithm

	SSD	ZNCC
Assumed temperature 1	0.018	0.993
CFD temperature 2	0.046	0.925
CFD temperature 3	0.044	0.927
CFD temperature 4	0.043	0.955

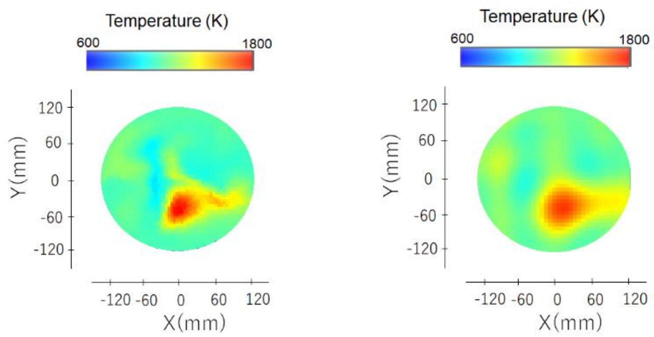

(a) CFD temperature 2 (b) CT reconstruction 2

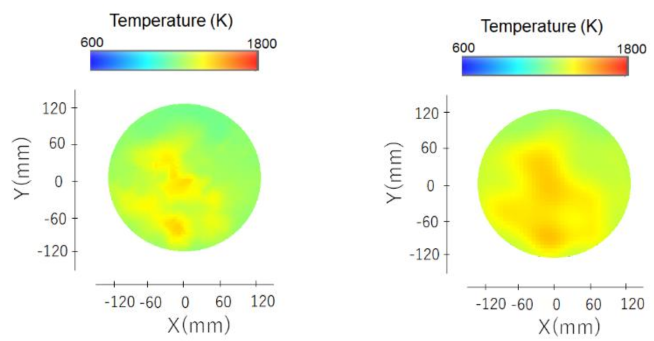

(c) CFD temperature 3 (d) CT reconstruction 3

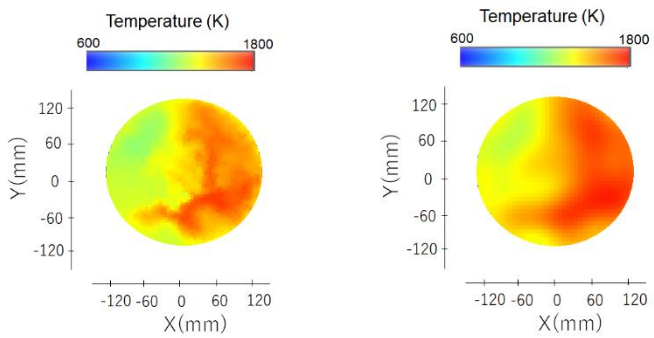

(e) CFD temperature 4 (f) CT reconstruction 4

Figure 6 Comparison of CFD temperature distributions and their reconstructed temperature distributions by 32-path CT-algorithm

4.2 Measurement of pulverized coal combustion using 32-path CT-TDLAS

The above reliable validation of CT-TDLAS demonstrated the feasibility of 2D temperature measurement using 32-path CT-TDLAS. Therefore, 2D temperature distribution in the pulverized coal combustion field was measured using this developed 32-path CT-TDLAS. According to the 32-path configuration, the 2D temperature distribution was plotted using 39×39 pixels (6mm resolution).

Two combustion states of CH_4 flame and pulverized coal flame were measured and discussed. Table 1 lists the experimental conditions for each combustion state. The CH_4 flow and air flow were introduced into CH_4 burner for CH_4 flame measurement in the combustion furnace. In the case of pulverized coal flame measurement, the fuels of CH_4 and pulverized coal were introduced into CH_4 burner and coal burner for combustion. CH_4 was used as a pilot gas for ignition and combustion. The CH_4 flame and pulverized coal flame were measured using 32-path CT-TDLAS respectively. 480 data, which were 480 ms time-series 2D temperature data, were analyzed in each flame condition. Figures 7 and 8 show the measured 2D temperature distribution and relative H_2O concentration distribution of CH_4 flame and pulverized coal with CH_4 flame. H_2O

concentration distribution was normalized by the maximum H_2O concentration distribution in each flame. The temperature distributions at the measurement plane can be reconstructed and observed, which illustrated different temperature distributions in CH_4 flame and pulverized coal flame. When comparing the average temperature distributions in Figure 7(a) and Figure 8(a), the temperature was higher in pulverized coal flame. These results indicate that the temperature increased when feeding coal to furnace. The input heat increased with the coal feed compared with that of only CH_4. Additionally, Figure 7(b) and Figure 8(b) show the temperature standard deviation of 480 data for CH_4 flame and pulverized coal flame. The standard deviation of temperature also increased with the coal feed and became large in the region with large temperature gradient. The combustion characteristic of gas fuel and pulverized coal are different due to the effect of component, morphology and so on. The combustion processes of pulverized coal usually consist of volatile devolatilization and combustion, carbon particles combustion after devolatilization, which are much more complex than that of CH_4 combustion. The temperature fluctuation of pulverized coal flame was larger because of coal particle effect including these combustion processes. One of the merits of CT-TDLAS method is the simultaneous measurement of temperature and concentration. 2D distributions of relative H_2O concentration in CH_4 flame and pulverized coal flame were reconstructed, as shown in Figure 7(c) and Figure 8(c).

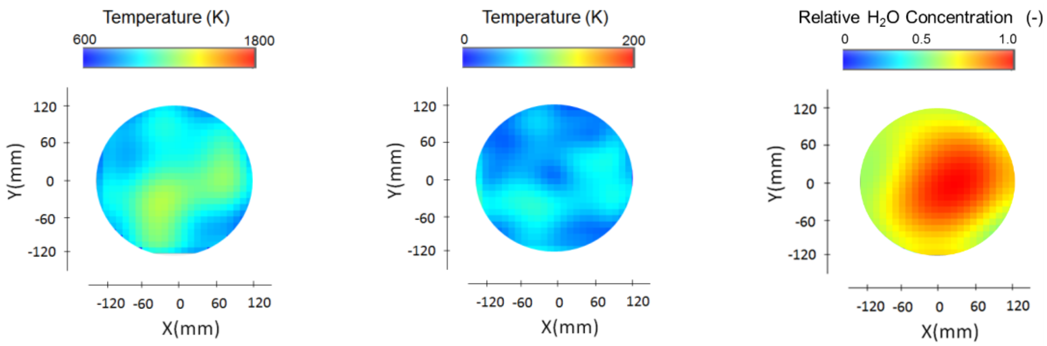

(a) Average temperature (b) Standard deviation (c) Relative H_2O concentration

Figure 7 Temperature and relative H_2O concentration distributions of CH_4 flame

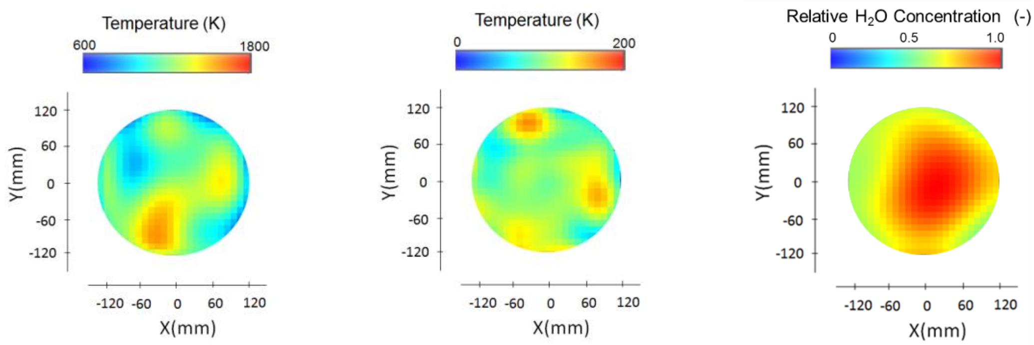

(a) Average temperature (b) Standard deviation (c) Relative H_2O concentration

Figure 8 Temperature and relative H_2O concentration distributions of pulverized coal flame

The time-series 2D temperature distribution was also detected with kHz time resolution. Time-series temperature distribution of pulverized coal flame is shown in Figure 9. The flame evolution of ms time scale was detected successfully in a turbulent coal combustion field. The variation of 2D temperature distribution can be investigated at different instants of time. The transient temperature field of combustion flame directly reflects the combustion mode and combustion stability. Due to the diversity, inhomogeneity, composition complexity of coal, the combustion laws of pulverized coal in coal combustion furnace can be further understood according to these measurement results. Simultaneity, the combustion furnace will be controlled in real time when the time-series temperature distribution is combined with combustion optimization and control strategy. The current results demonstrate that 2D temperature distribution of pulverized coal flame can be detected using 32-path CT-TDLAS, which shows CT-TDLAS applicability to dusty combustion fields in real time for combustion phenomena investigation.

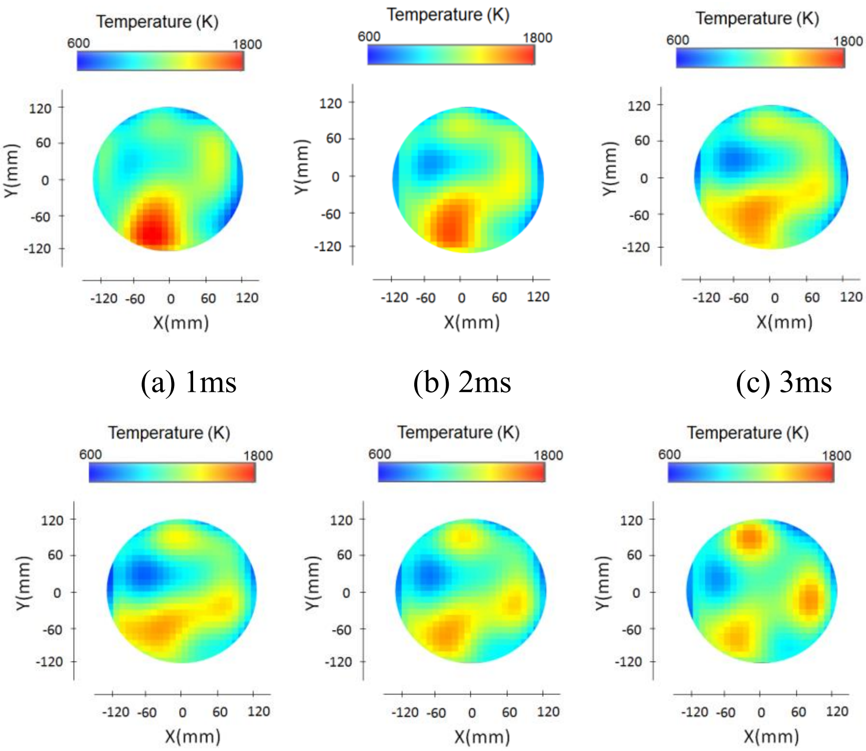

(a) 1ms (b) 2ms (c) 3ms

(d) 4ms (e) 5ms (f) 6ms

Figure 9 Time-series 2D temperature distribution of pulverized coal flame

5. Conclusions

It is of great importance to diagnose and control combustion process for coal combustion in real time. The 2D temperature measurement method using CT-TDLAS was developed for a pulverized coal combustion furnace. The temperature measurement accuracy of TDLAS using H_2O absorption spectra and the 2D reconstruction accuracy of developed 32-path CT-algorithm were evaluated to verify its reliability for 2D temperature measurement. The contrast analysis for measured results of average temperature and temperature standard deviation between CH_4 flame and pulverized coal flame proved the complexity of pulverized coal combustion. The time-series 2D temperature distribution was successfully reconstructed with ms time scale in the pulverized coal combustion conditions. It is demonstrated that this CT-TDLAS method enables the real-time 2D temperature measurement in dusty combustion fields such as coal burners. Potential extension of this research in the future is to investigate a monitoring and control system coupled with laser measurement and numerical simulation for combustion diagnostics.

Acknowledgement

This work was supported by the CT-TDLAS consortium operated by Tokushima University.

References

[1] Deguchi Y. Industrial applications of laser diagnostics, New York: CRS Press Taylor & Francis; 2011.

[2] Deguchi Y, Noda M, Fukuda Y, Ichinose Y, Endo Y, Inada M., et al. Industrial applications of temperature and species concentration monitoring using laser diagnostics. Meas Sci Technol 2002; 13(10): R103-R115. https://doi:10.1088/0957-0233/13/10/201.

[3] Zaatar Y, Bechara J, Khoury A, Zaouk D, Charles JP. Diode laser sensor for process control and environmental monitoring. Appl Energy 2000; 65: 107-113. https://doi:10.1016/S0306-2619(99)00090-2.

[4] Liu X, Jeffries JB, Hanson RK, Hinckley KM, Woodmansee MA. Development of a tunable diode laser sensor for measurements of gas turbine exhaust temperature. Appl Phys B 2006; 82(3): 69-478. http://doi:10.1007/s00340-005-2078-9.

[5] Sur R, Sun K, Jeffries JB, Socha JG, Hanson RK. Scanned-wavelength-modulation-spectroscopy sensor for CO, CO_2, CH_4 and H_2O in a high-pressure engineering-scale transport-reactor coal gasifier. Fuel 2015; 150: 102-111. https://doi:10.1016/j.fuel.2015.02.003.

[6] Burkle S, Becker LG, Dreizler A, Wagner S. Experimental investigation of the flue gas thermochemical composition of an oxy-fuel swirl burner. Fuel 2018; 231: 61-72. https://doi:10.1016/j.fuel.2018.05.039.

[7] Yamakage M, Muta K, Deguchi Y, Fukada S, Iwase T, Yoshida T. Development of direct and fast response exhaust gas measurement. SAE Paper 2008; 20081298.

[8] Pal S, McCann H. Auto-digital gain balancing: a new detection scheme for high-speed chemical species tomography of minor constituents. Meas Sci Technol 2011; 22(11): 115304 (13pp). https://doi:10.1088/0957-

0233/22/11/115304.

[9] Wright P, Terzijaa N, Davidsona JL, Garcia-Castillo S, Garcia-Stewart C, Pegrumb S, et al. High-speed chemical species tomography in a multi-cylinder automotive engine. Chem Eng J 2010; 158(1): 2-10. https://doi:10.1016/j.cej.2008.10.026.

[10] Deguchi Y, Kamimoto T, Wang ZZ, Yan JJ, Liu JP, Watanabe H, et al. Applications of laser diagnostics to thermal power plants and engines. Appl Therm Eng 2014; 73(2): 1453-1464. https://doi:10.1016/j.applthermaleng.2014.05.063.

[11] Ma L, Li X, Sanders ST, Caswell AW, Roy S, Plemmons DH, et al. 50-kHz-rate 2D imaging of temperature and H_2O concentration at the exhaust plane of a J85 engine using hyperspectral tomography. Opt Express 2013; 21(1): 1152-1162. https://doi:10.1364/OE.21.001152.

[12] Wang F, Cen KF, Li N, Jeffries JB, Huang QX, Yan JH, et al. Two-dimensional tomography for gas concentration and temperature distributions based on tunable diode laser absorption spectroscopy. Meas Sci Technol 2010; 21: 045301 (10pp). https:// doi:10.1088/0957-0233/21/4/045301.

[13] Ma L, Cai W. Numerical investigation of hyperspectral tomography for simultaneous temperature and concentration imaging. Appl Opt 2008; 47(21): 3751-3759. https://doi:10.1364/AO.47.003751.

[14] An X, Kraetschmer T, Takami K, Sanders ST, Ma L, Cai W, et al. Validation of temperature imaging by H_2O absorption spectroscopy using hyperspectral tomography in controlled experiments. Appl Opt 2011; 50(4): A29-A37. https://doi:10.1364/AO.50.000A29.

[15] Samuel JG, Johannes E, Scott TS, Steven W, Kyle JD. Multiparameter gas sensing with linear hyperspectral absorption tomography. Meas Sci Technol 2019; 30: 105401(16pp). https://doi.org/10.1088/1361-6501/ab274b.

[16] Cai W, Kaminski CF. Tomographic technique for the simultaneous imaging of temperature, chemical species, and pressure in reactive flows using absorption spectroscopy with frequency agile Lasers. Appl Phys Lett 2014; 104: 034101. https://doi.org/10.1063/1.4862754.

[17] Kamimoto T, Deguchi Y, Zhang N, Nakao N, Takagi T, Zhang Z. Real-time 2D concentration measurement of CH_4 in oscillating flames using CT tunable diode laser absorption spectroscopy. Journal of Applied Nonlinear Dynamics 2015; 4(3): 295-303.

[18] Kamimoto T, Deguchi Y, Kiyota Y. High temperature field application of two dimensional temperature measurement technology using CT tunable laser absorption spectroscopy. Flow Meas Instrum 2015; 46: 51-57. https://doi:10.1016/j.flowmeasinst.2015.09.006.

[19] Tsekenis SA, Tait N, McCann H. Spatially resolved and observer-free experimental quantification of spatial resolution in tomographic images. Rev Sci Instrum 2015; 86(3): 035104. https://doi:10.1063/1.4913922.

[20] Jeon MG, Deguchi Y, Kamimoto T, Doh DH, Cho GR. Performances of new reconstruction algorithms for CT-TDLAS (computer tomography-tunable diode laser absorption spectroscopy). Appl Therm Eng 2017; 115: 1148-1160. https://doi:10.1016/j.applthermaleng.2016.12.060.

[21] Rothman LS, Gordon IE, Babikov Y, Barbe A, Chris Benner D, Bernath PF, et al. The HITRAN 2012 molecular spectroscopic database. Journal of Quantitative Spectroscopy & Radiative Transfer 2013, 130, 4-50. https://doi.org/10.1016/j.jqsrt.2013.07.002.

[22] Nelder JA, Mead R. A simplex method for function minimization. The Computer Journal 1965; 7(4): 308-313. https://doi:10.1093/comjnl/7.4.308.

[23] Po LM, Guo K. Transform-domain fast sum of the squared difference computation for H.264/AVC rate-distortion optimization. IEEE Trans Circuits Syst Video Technol 2007; 17(6): 765-773. https://doi:10.1109/TCSVT.2007.896663.

[24] Pan B. Recent progress in digital image correlation. Exp Mech 2011; 51: 1223-1235. https://doi:10.1007/s11340-010-9418-3.

[25] Kamimoto T, Deguchi Y. 2D temperature detection characteristics of engine exhaust gases using CT tunable diode laser absorption spectroscopy. Int J Mech Syst Sci Eng 2015; 1: 109. http://dx.doi.org/10.15344/ijmse/2015/109.

[26] Muto M, Watanabe H, Kurose R, Komori S, Balusamy S, Hochgreb S. Large-eddy simulation of pulverized coal jet flame - Effect of oxygen concentration on NOx formation. Fuel 2015; 142: 152-163. https://doi:10.1016/j.fuel.2014.10.069.

[27] Watanabe H, Tanno K, Umetsu H, Umemoto S. Modeling and simulation of coal gasification on an entrained flow coal gasifier with a recycled CO_2 injection. Fuel 2015; 142: 250-259. https://doi:10.1016/j.fuel.2014.11.012.

[28] Ahn S, Tanno K, Watanabe H. Numerical analysis of particle dispersion and combustion characteristics on a piloted coaxial pulverized coal jet flame. Appl Therm Eng 2017; 124: 1194-1202. https://doi:10.1016/j.applthermaleng.2017.06.103.